The Journal of Neuroscience, February 1995, 15(2): 1341–1351

Postnatal Development of $GABA_A$ Receptor Function in Somatosensory Thalamus and Cortex: Whole-Cell Voltage-Clamp Recordings in Acutely Isolated Rat Neurons

Kwang-Soo Oh,[1,a] Chang-Joong Lee,[1,b] John W. Gibbs,[2] and Douglas A. Coulter[1,3]

Departments of [1]Neurology and [2]Anatomy, Medical College of Virginia, and [3]MCV Comprehensive Epilepsy Institute of Virginia Commonwealth University, Richmond, Virginia 23298-0599

GABAergic inhibition synchronizes oscillatory activity in the thalamocortical system. To understand better the role of this neurotransmitter in generation of thalamocortical rhythmicity, the postnatal development of GABAergic function mediated through activation of $GABA_A$ receptors was studied in thalamus and cortex. GABA-evoked chloride currents were recorded in dissociated rat cortical and thalamic neurons during postnatal development. Kinetic fits of GABA concentration/response relationships revealed developmental and regional alterations in the potency of GABA. Early in postnatal development (p5–p8), both thalamic and cortical neurons exhibited reduced potency of GABA (27–31 μM K_D). Potency increased by p18–p25 in thalamic and cortical neurons (19–22 μM K_D), to a level maintained in adult thalamic neurons. Adult cortical neurons exhibited reduced potency of GABA (40 μM K_D). Benzodiazepine modulation of $GABA_A$ currents was also studied. Kinetic analyses of benzodiazepine augmentation of $GABA_A$ currents were best fitted assuming two effective sites with different affinities for clonazepam. The high-affinity site (K_D of 0.05–0.27 nM) showed little variation with development in cortical neurons, contributing about 16–23% potentiation at all postnatal ages. Developing thalamic neurons (p5–p25) showed similar potency and efficacy of the high-affinity benzodiazepine site to cortical neurons. High-affinity benzodiazepine effects disappeared in adult thalamic neurons. A lower-affinity benzodiazepine site (25–50 nM K_D) was greater in efficacy in cortical neurons compared to thalamic neurons at all ages, with efficacy ranging from 50% to 110% in cortex and from 20% to 60% in thalamus. Knowledge of developmental and regional alterations in $GABA_A$ receptor function may aid in understanding mechanisms involved in generation and control of normal and pathological thalamocortical rhythms.

[Key words: thalamus, cortex, postnatal development, GABA, voltage clamp, generalized absence epilepsy, thalamocortical rhythmicity, benzodiazepines, barbiturates]

In the thalamocortical system, the tightly interconnected synaptic circuitry and oscillatory voltage-dependent ionic conductances within neurons comprising the circuit predispose the system to support phasic bursting activity as one of two main behavioral states. In this system, GABAergic inhibition synchronizes and drives the phasic oscillatory activity that generates normal and pathological rhythms like sleep spindles (SSs) and the spike-wave discharges (SWDs) recorded in the electroencephalogram of children experiencing generalized absence (GA) seizures (Purpura and Cohen, 1962; Anderson and Sears, 1964; Steriade et al., 1985; reviewed in Gloor and Fariello, 1988; Steriade and Llinás, 1988). The critical role of GABAergic inhibition in synchronizing thalamocortical oscillations is particularly evident in rodent genetic models of GA, in which thalamic infusion of GABAergic agonists trigger or exacerbate SWDs (are proconvulsant), while GABAergic antagonists block or reduce SWDs, that is, are anticonvulsant (Liu et al., 1991, 1992; Hosford et al., 1992).

The thalamocortical system is the principal pathway transferring information from the periphery to the cortex, and has been extensively studied in many species. Thalamic sensory nuclei send axonal projections to neocortex, and receive feedback projections from the same cortical area. Thalamocortical and corticothalamic axons also send collaterals to nucleus reticularis thalami (NRT), a GABAergic nucleus surrounding the thalamus (Houser et al., 1980; Jones, 1985). This nucleus provides inhibitory feedback to thalamus. GABAergic inhibition originating from NRT acts as the pacemaker for thalamocortical rhythms (Steriade et al., 1985, 1987; Huguenard and Prince, 1994; reviewed in Steriade and Llinás, 1988). During SSs, NRT neurons fire repetitive bursts, which trigger large IPSPs in thalamic neurons. Thalamic neurons then fire large bursts of action potentials on the IPSP decay, due to deinactivation, and subsequent activation, of the low-threshold calcium spike (LTS) by the IPSP (Deschênes et al., 1982; Llinás and Jahnsen, 1982; Jahnsen and Llinás, 1984). This LTS then reinitiates activity, and is critically important in generation of thalamocortical oscillations. Block of this LTS conductance may be a mechanism of action of many drugs effective in controlling the pathological thalamocortical rhythms of GA (Coulter et al., 1989b,c, 1990a).

$GABA_A$ and $GABA_B$ receptors are distributed throughout the thalamocortical system of rodents (Bowery et al., 1987; Olsen et al., 1990), and GAD-positive terminals have been described

Received Mar. 23, 1994; revised Aug. 1, 1994; accepted Aug. 10, 1994.

We thank George P. Nanos III for excellent technical support. This work was supported by a Milken Family Award from the American Epilepsy Society (to D.A.C.), by NIH-NINDS Grant R29 NS-31000 (D.A.C.), by the Sophie and Nathan Gumenick Foundation Neuroscience and Alzheimer's Research Fund (D.A.C.), by a Wonkwang University grant (K.-S.O.), by a grant from the Ministry of Education of Korea (C.-J.L.), and by the MCV Foundation (J.W.G.).

Correspondence should be addressed to Dr. Douglas A. Coulter, Department of Neurology, P.O. Box 980599, Medical College of Virginia, Richmond, VA 23298-0599.

[a]Present address: Department of Pediatrics, Division of Child Neurology, Wonkwang University School of Medicine, 344-2 Shinyong-Dong Iri-City, Chonbuk, Korea 570-749.

[b]Present address: Department of Biology, Inha University, 253 Yonghyun-dong, Nam-gu, Inchon, Korea 402-751.

in several thalamic nuclei (Houser et al., 1980). However, recent *in situ* mRNA hybridization experiments have demonstrated a pronounced differential regional and developmental distribution within the cortex and thalamus of several of the mRNAs coding for specific subunits of the $GABA_A$ receptor hetero-oligomeric complex (Olsen and Tobin, 1990; Wisden et al., 1992). In particular, mRNA coding for the γ subunit of the $GABA_A$ receptor, which confers benzodiazepine sensitivity onto GABAergic responses (Pritchett et al., 1989), was noticeably reduced in rodent thalamus (Wisden et al., 1992; but see Araki et al., 1992; Persohn et al., 1992).

Because of the importance of GABAergic inhibition in generation of thalamocortical rhythmicity with the associated clinical significance of these rhythms, we were interested in functionally characterizing the properties and postnatal development of $GABA_A$ receptors on cortical and thalamic neurons, using patch-clamp recording techniques in acutely isolated neurons.

Materials and Methods

Acute isolation of neurons. All experiments were performed on thalamic and cortical neurons, acutely isolated from the 5–74-d-old rats using methods originally described by Kay and Wong (1986), modified as described in Coulter et al. (1989a). Animals were anesthetized with halothane and decapitated, and the brains rapidly removed and placed into chilled, oxygenated (95% O_2/5% CO_2) artificial cerebrospinal fluid (ACSF), composed of (in mM) NaCl, 130; KCl, 3; NaH_2PO_4, 1.25; $MgCl_2$, 2; $CaCl_2$, 2; $NaHCO_3$, 26; and dextrose, 10. The brain was then blocked and glued (with cyanoacrylate glue) onto the stage of Vibratome (Lancer 1000, TPI, Inc., St. Louis, MO) and 400 μm coronal sections were prepared containing somatosensory thalamus and cortex. These slices were then incubated for 1 hr following dissection in oxygenated medium containing (in mM) NaCl, 120; KCl, 5; $MgCl_2$, 1; $CaCl_2$, 1; glucose, 25; and piperazine-*N,N'*-bis[2-ethanesulfonic acid] (PIPES), 20; with the pH adjusted to 7.0 with NaOH. Slices were then incubated a further 30–60 min in PIPES medium containing 3 mg/ml Sigma protease XXIII, thoroughly rinsed, and incubated another 45 min in PIPES medium prior to mechanical dissociation. Mechanical dissociation was accomplished by cutting 1 mm^2 chunks of appropriate areas (ventrobasal complex of thalamus and somatosensory cortex) from the enzymed slices. These chunks were then triturated through a series of fire-polished Pasteur pipettes, and dispersed neurons were plated in *N*-2-hydroxyethylpiperazine-*N'*-2-ethane sulfonic acid (HEPES) medium onto 35 mm culture dishes, and stored in an oxygenated chamber prior to recording. The external recording solution (HEPES medium) was composed of (in mM) NaCl, 155; KCl, 3; $MgCl_2$, 1; $CaCl_2$, 3; tetrodotoxin, 0.0005; and HEPES-Na^+, 10; with pH adjusted to 7.4 with NaOH. On most experimental days, neurons from both thalamus and cortex of the same animal were recorded, facilitating comparison of $GABA_A$ response properties between brain areas. The ventrobasal complex of the thalamus could easily be distinguished from the surrounding NRT, and care was taken to exclude NRT from areas to be dissociated. Using these methods, it has been verified immunohistochemically that very few GABAergic neurons are isolated from the ventrobasal complex, confirming the exclusion of NRT from the isolated thalamic neuron population (Huguenard and Prince, 1992). To reduce variability further in recordings within cortical neurons, only medium to large, pyramidal-shaped cortical neurons were employed for study.

Voltage-clamp recordings. Whole-cell patch-clamp recording techniques were similar to those described by Hamill et al. (1981). Electrodes (6–8 MΩ resistance) were pulled on a Narishige PP-83 microelectrode puller using a two-stage pull and thin-walled borosilicate capillary glass. The intracellular (pipette) solution contained (in mM) Trizma phosphate (dibasic), 100; Trizma base, 28; ethylene glycol bis-(β-aminoethylether)-*N,N,N',N'*-tetraacetic acid, 11; $MgCl_2$, 2; $CaCl_2$, 0.5; and Na_2-ATP, 4; with pH adjusted to 7.35 with NaOH. The pipette solution also contained an intracellular ATP reconstitution consisting of 50 U/ml creatinine phosphokinase and 22 mM phosphocreatinine (Forscher and Oxford, 1985; Mody et al., 1988). This reconstitution system maintained energy stores of the neurons, and prevented rundown of GABA currents, which has previously been described in acutely isolated neurons (Huguenard and Alger, 1986; Stelzer et al., 1988). The maintenance solution was used to fill the shank of the electrode, but was omitted from the solution that was used to back-fill the tip of the electrode, because it was found that gigaohm seals were difficult to obtain with protein in the tip solution. Recordings were amplified using an Axopatch 200A amplifier (Axon Instruments, Burlingame, CA), and filtered at 5 kHz with a 4-pole Bessel filter before digitization. All data were displayed on a chart recorder on line (model 2107, Gould, Cleveland, OH; frequency response DC to 50 Hz), and stored on videotape following digitization (at 44 kHz) with a PCM interface (Neurodata Instrument Co., New York, NY). For subsequent off-line analysis, data were played back on a chart recorder with a frequency response of DC to 2500 Hz (Astro-Med DASH IV, Warwick, RI).

Drug concentrations and method of application. All drug solutions were freshly prepared daily, except for GABA, which was prepared as a 1 M stock solution and then diluted to the final concentration in the external solutions. Clonazepam was first dissolved in dimethyl sulfoxide (DMSO) at 10 mM. The maximum concentration of DMSO used in cellular perfusions was <0.001%. During clonazepam experiments, all perfusion barrels (including control and wash barrels) contained DMSO to minimize any potential artifacts. Application of DMSO alone (0.1%) did not alter GABA responses. The applied drug concentrations were as follows: GABA (Sigma, St. Louis, MO), 1–3000 μM; clonazepam (Sigma), 0.01–1000 nM; phenobarbital (Sigma), 50 μM; bicuculline (Research Biochemicals Inc., Natick, MA), 10 μM.

Solution changes were accomplished using the "sewer pipe" perfusion technique (Yellen, 1982; Huguenard et al., 1991), in which several solutions flow out of parallel Teflon tubes (0.2 mm i.d.; Cole Parmer Instrument Co., Niles, IL) in a laminar pattern. Rapid (<100 msec) and complete solution changes at a constant flow rate were then effected by moving the tube assembly in relation to the neuron under study. While initiating recording from neurons, the cell was perfused with control external solution, with the barrels placed about 50 μm away from the tip (mouth) of each tube. After breaking the seal and allowing approximately 2–5 min to pass to establish stable leak currents (0 to −250 pA), GABA was applied for 8–10 sec, and washed out with control external solution for 100 sec. The cell was then pretreated with test drugs without GABA solutions for 100 sec, and then test solutions were applied, together with GABA. Drug effects were expressed as percentage effect on GABA-evoked outward currents, recorded at −20 mV V_{HOLD}. Experiments were performed at room temperature (22–24°C)

Statistics. All data were analyzed by calculating the current amplitude of test solutions relative to currents evoked by GABA application alone and only reversible effects were analyzed. All data are expressed as mean ± 1 standard error unless otherwise specified. Significance was tested using the two-tailed Student's *t* test. Both the GABA concentration/response and the clonazepam concentration/GABA augmentation relationships were fitted by the Marquardt-Levenberg nonlinear least squares method (ORIGIN, MicroCal Software, Inc., Northhampton, MA).

Results

GABA-induced currents

Bath application of 10 μM GABA to cortical neurons (postnatal day 25, p25) elicited a current with a reversal potential (E_{GABA}) of −63 ± 5.2 mV (mean ± SE, n = 5), accompanied by an increase in conductance (Fig. 1*A–C*). This reversal potential was close to that for a chloride current derived from the Goldman-Hodgkin-Katz equation (Goldman, 1943; Hodgkin and Katz, 1949). Under the ionic conditions of this study, assuming a phosphate-to-chloride permeability ratio of 0.025 (Bormann et al., 1987), and an activity coefficient of 0.75 for the 166 mM external chloride solution, the calculated E_{GABA} was −70 mV.

The GABA-induced chloride current showed pronounced outward rectification in both cortical and thalamic neurons (Fig. 1*B*), as has been previously described in other neurons (Segal and Barker, 1984; Barker and Harrison, 1988; Coulter et al., 1990b). This current and accompanying conductance increase elicited by 10 μM GABA were reduced or blocked by bath application of 10 μM bicuculline (91.1 ± 3.8% block, mean ± SE, n = 5, in p66 thalamic neurons; 90.5 ± 2.5% block, n = 5, in p66 cortical neurons; Fig. 1*C*). In contrast, the peak GABA

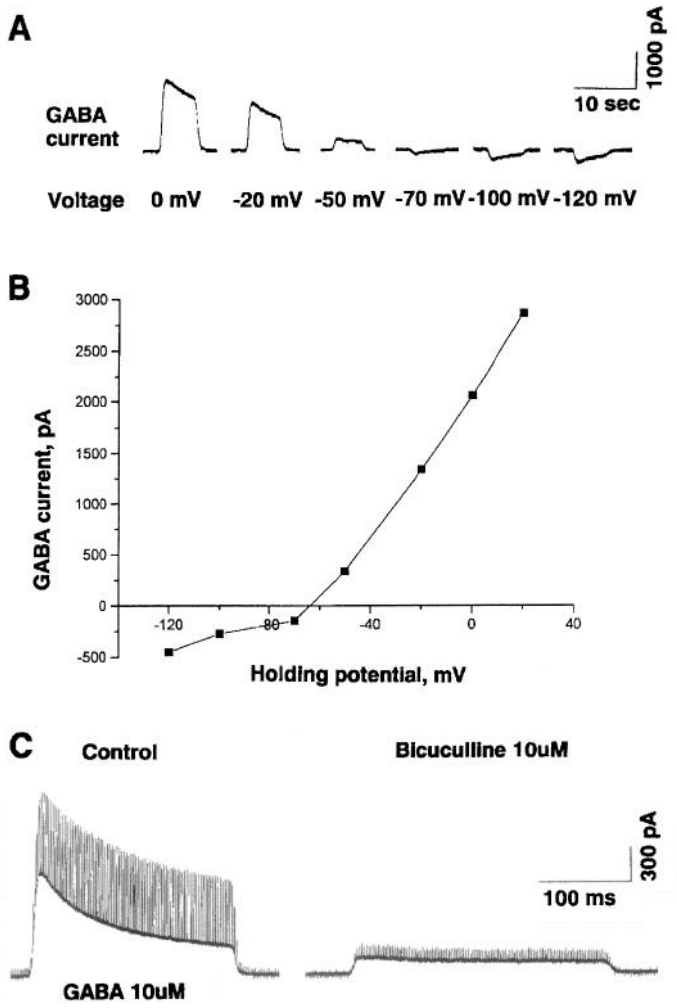

Figure 1. Properties of GABA-evoked currents are typical of $GABA_A$-mediated Cl^- conductances. *A*, Traces illustrating how the amplitude of the GABA-evoked currents varied with the holding potential at which the neuron was voltage-clamped. The holding potentials are displayed below each trace. Data are from a p25 cortical neuron. *B*, Plot of the reversal potential for the traces depicted in *A*. Note the reversal of the GABA current at −63 mV, and the pronounced outward rectification. *C*, Block of both GABA (10 μM)-evoked outward current and associated conductance increase by 10 μM bicuculline. The conductance of the cell before, during, and after GABA application was valuated using continually repeating 5 mV conductance pulses, which evoked consistently larger currents (indicating higher membrane conductance) during GABA application. Data are from a p66 cortical neuron.

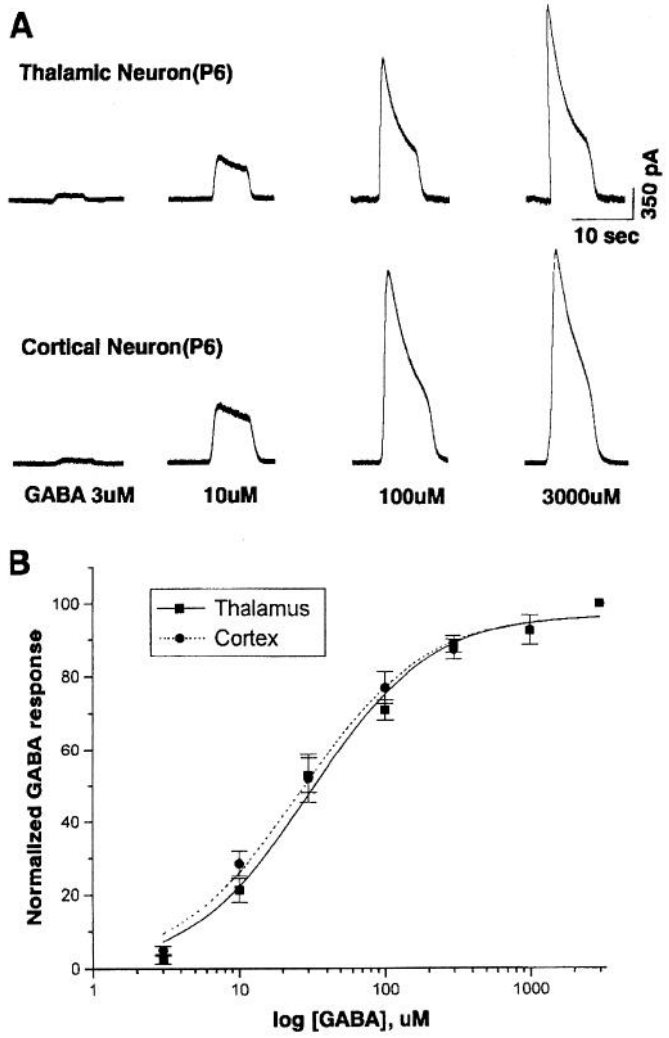

Figure 2. GABA concentration/response relationship for p5–p8 rat thalamic and cortical neurons. *A*, Traces illustrating the response of a thalamic (*top*) and a cortical neuron (*bottom*) to four concentrations of GABA, while the neuron was voltage-clamped at −20 mV. The concentration of GABA eliciting the current appears below each trace. Both neurons are from the same animal, a p6 rat. *B*, Log/linear plot of the concentration of GABA against the mean ± 1 SE response, normalized to the response elicited by application of 3 mM GABA. Curves are unbiased nonlinear least squares fits of the data (fit parameters are in Table 1). Note the similar potency of GABA in p5–p8 cortical and thalamic neurons.

current elicited by 3 mM GABA application (receptor saturating levels of GABA; see Figs. 2–4) was not blocked by application of 10 μM bicuculline, consistent with competitive inhibition of GABA responses by bicuculline (not shown).

Development of GABA responses in cortical and thalamic neurons

Figures 2–4 show the GABA-induced chloride current for 3 postnatal age groups: p5–p8 (Fig. 2), p18–p25 (Fig. 3), and p60–p74 (Fig. 4) at a holding potential of −20 mV. GABA concentration/response curves obtained derived from GABA application in the concentration range from 1 μM to 3 mM were fitted using a nonlinear least squares method (Marquardt-Levenberg method). The equation used to fit the GABA concentration/response relationship was

$$I = I_{max}C^n/(C^n + K_D^n), \quad (1)$$

where C is the GABA concentration, I is the current elicited by a given GABA concentration normalized to the GABA current elicited by application of 3 mM GABA in the same neuron, I_{max} is the maximal GABA current expressed as a percentage of the 3 mM GABA response, K_D is the GABA concentration eliciting half-maximal current, and n is the Hill coefficient. Nonlinear least squares fits of the data gave K_D values and Hill coefficients for each age, as are shown in Table 1.

The overall efficacy (or maximal effect) of GABA on cortical and thalamic neurons was the same for all three developmental stages. The potency (or K_D) of GABA acting at $GABA_A$ receptors varied with postnatal development, and between brain areas.

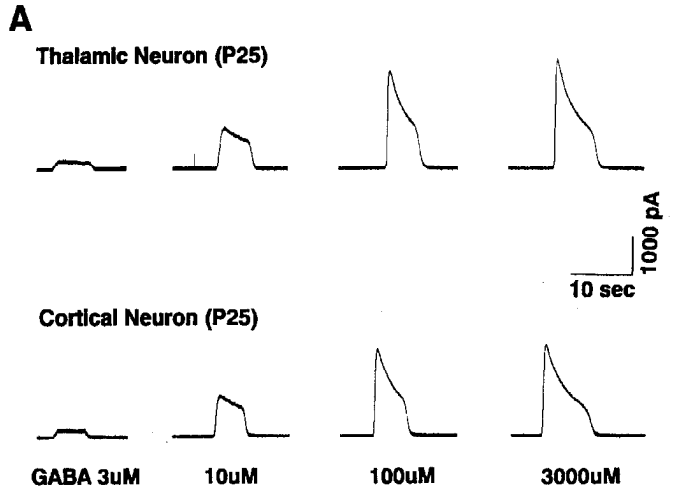

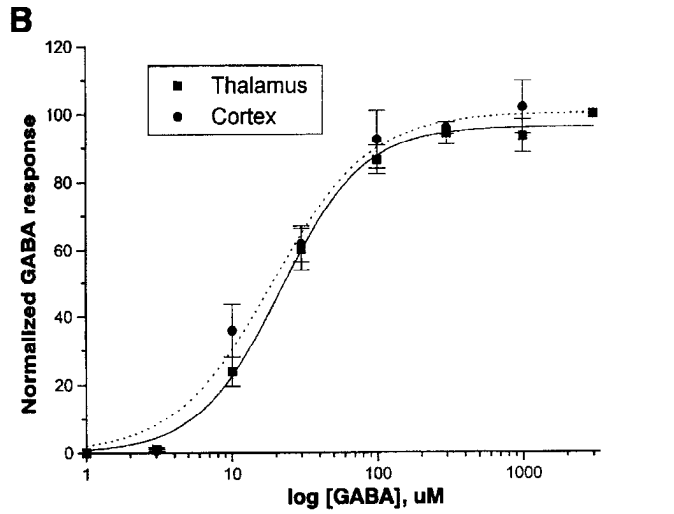

Figure 3. GABA concentration/response relationship for p18–p25 rat thalamic and cortical neurons. *A*, Traces illustrating the response of a thalamic (*top*) and a cortical neuron (*bottom*) to four concentrations of GABA, while the neuron was voltage-clamped at −20 mV. The concentration of GABA eliciting the current appears below each trace. Both neurons are from the same animal, a p25 rat. *B*, Log/linear plot of the concentration of GABA against the mean ± 1 SE response, normalized to the response elicited by application of 3 mM GABA. Curves are unbiased nonlinear least squares fits of the data (fit parameters are in Table 1). Note the similar potency of GABA in p18–p25 cortical and thalamic neurons.

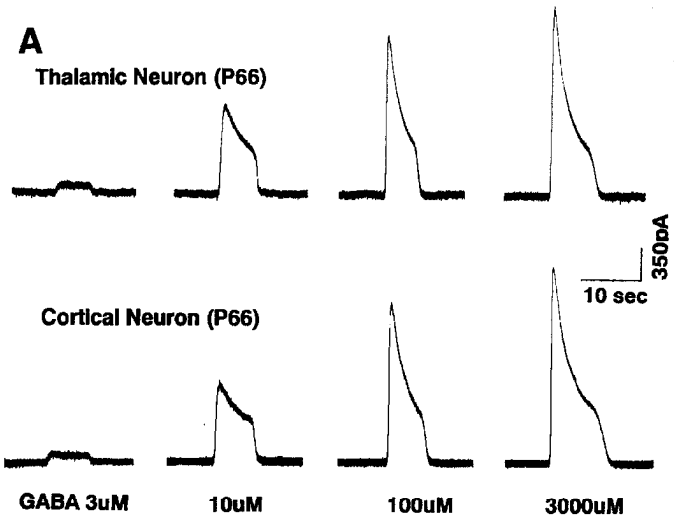

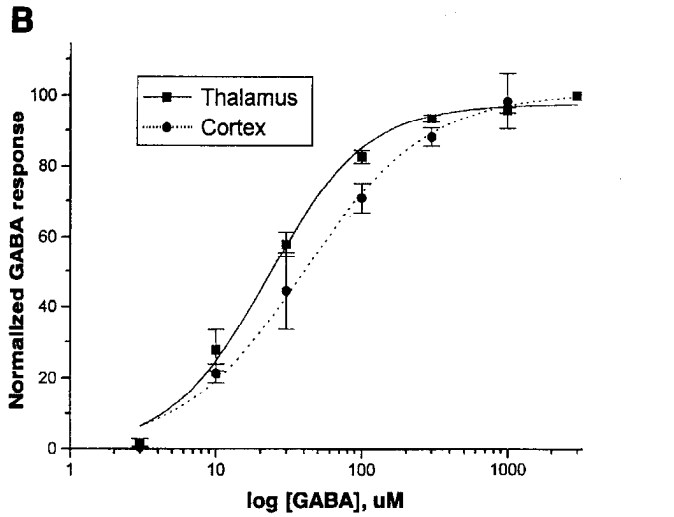

Figure 4. GABA concentration/response relationship for adult (p60–p75) rat thalamic and cortical neurons. *A*, Traces illustrating the response of a thalamic (*top*) and a cortical neuron (*bottom*) to four concentrations of GABA, while the neuron was voltage-clamped at −20 mV. The concentration of GABA eliciting the current appears below each trace. Both neurons are from the same animal, a p66 rat. *B*, Log/linear plot of the concentration of GABA against the mean ± 1 SE response, normalized to the response elicited by application of 3 mM GABA. Curves are unbiased nonlinear least squares of the data (fit parameters are in Table 1). Note the reduced potency of GABA in adult cortical neurons relative to thalamic neurons.

The concentration of GABA exhibiting half-maximal effect diminished in the following sequence in cortical neurons: p60–p74 > p5–p8 > p18–p25. This developmental alteration in GABA potency was different in thalamic neurons, with GABA having the lowest potency in p5–p8 neurons, and higher potency in p18–p25 and p60–p74 neurons, with both older developmental stages being equal in GABA potency. There was little difference in the relative potency of GABA responses in cortical and thalamic neurons at a given age, except in adult neurons (p60–p74), where GABA was higher in potency in thalamus relative to cortex (Table 1).

The current density of GABA receptor–mediated responses increased with postnatal development, in both thalamic and cortical neurons. There was no difference in GABA current density between thalamus and cortex at any developmental stage. Current density was calculated based on the maximal response of a neuron to 3 mM GABA, which was then divided by the membrane capacitance of the cell, read directly off the capacitance compensation potentiometer on the patch amplifier. Capacitance readings using this method are in reasonable agreement with membrane capacitance measurements derived from integrating the current response to a small depolarizing step [16.0–18.0 pF in acutely isolated p5–p25 thalamic neurons read off the amplifier capacitance compensation potentiometer in the present study (Table 2), compared to 17.5 ± 0.63 pF calculated via integration in acutely isolated p7–p15 thalamic neurons in Huguenard et al. (1991)]. Assuming a capacitance/membrane

Table 1. GABA concentration/response fit parameters for cortical and thalamic neurons of various postnatal ages

	Cortex			Thalamus		
Age	Maximal current	Hill coefficient	K_D (μM)	Maximal current	Hill coefficient	K_D (μM)
p5–p8	97.1 ± 2.8	1.01 ± 0.11	26.6 ± 3.4	96.9 ± 3.8	1.07 ± 0.17	31.0 ± 5.1
p18–p25	100.4 ± 3.0	1.34 ± 0.20	18.9 ± 2.4	96.3 ± 1.6	1.52 ± 0.14	21.6 ± 1.5
p60–p74	100.8 ± 3.0	1.03 ± 0.11	40.3 ± 4.9	97.7 ± 2.2	1.26 ± 0.14	22.8 ± 2.2

All values are ±1 SE. Number of neurons recorded: p5–p8, 35 cortex, 31 thalamus; p18–p25; 50 cortex, 60 thalamus; p60–p74, 81 cortex, 44 thalamus.

area relationship of 1 μF/cm^2 (or 0.01 pF/μm^2), the GABA current densities for the various neuron types and ages are enumerated in Table 2. With a GABA single-channel conductance of 20–30 pS, a 50 mV driving force, and a maximal probability of GABA channel opening of 0.83 at mM GABA concentrations (Newland et al., 1991), these current densities would correspond to a GABA channel density of 1.3–1.9 channels/μm^2 in p5–p8 neurons, and 1.6–2.5 channels/μm^2 in adult neurons. This is derived using the equation $I = Nip$, where I is the mean current per μm^2 (from Table 2), i is the single-channel current computed from the single-channel conductance and the driving force, and p is the probability of channel opening, assumed to be 0.83 for the concentration of GABA employed (Newland et al., 1991). Since perhaps one-third of the neuron's membrane may be inaccessible to applied GABA due to its close apposition to the surface of the petri dish, this channel density estimate probably underestimates the actual channel density, although these estimates are adequate for comparison of relative channel densities across developmental stages and brain areas. Unlike GABA current density, the capacitance of the cells decreased with development (Table 2). This surprising finding was probably artifactual and related to the ease with which cells were isolated by the enzymatic/mechanical techniques employed in the present study. The youngest cells (p5–p8) tended to isolate more easily, and also tended to have longer dendrites attached to the soma. The ease of isolation decreased with increasing age of the brain, which was associated with a decreased dendritic area, although the soma size increased with increasing age of the cells. The overall decreased membrane area in older neurons, coupled with an increased GABA current density in neurons from older animals tended to keep the peak GABA currents (recorded in response to 3 mM GABA application) relatively uniform in size (Table 2), The overall desensitization of the GABA response (to 3 mM GABA) decreased with postnatal development in cortical neurons, but not in thalamic neurons (Table 2). Desensitization was expressed as the ratio of the GABA current amplitude 8 sec after onset of exposure to 3 mM GABA to the peak GABA current and was expressed as a percentage. By this type of measure, cells that had a higher desensitization percentage value exhibited less desensitization than cells with a lower percentage value. Cortical neurons at all ages showed significantly more desensitization than did thalamic neurons of the same age (Table 2).

Effects of clonazepam on GABA-induced Cl^- currents in cortical and thalamic neurons of various ages

When GABA (1–3000 μM) was applied to neurons using a concentration-clamp apparatus and a V_{HOLD} of −20 mV, the concentration/response curve of GABA-induced currents was sigmoidal (e.g., Figs. 2–4). As the concentration of GABA increased, the Cl^- current began to exhibit more and more rapid desensitization. To examine benzodiazepine potentiation of GABA currents, a concentration of 10 μM GABA was chosen, since this concentration was on the rising phase of the concentration/response curve for all ages and brain areas and exhibited a minimum degree of desensitization. This concentration of GABA elicited $GABA_A$ currents that were the following percentage of maximal current: p5–p8 thalamus 18.5%, cortex 21.8%; p18–p25 thalamus 16.2%, cortex 14.4%; and p60–p74 thalamus 19.6%, cortex 14.2%. To minimize possible errors in calculating potentiation of GABA responses in the presence of benzodiazepine, the drift rate of the GABA currents was calculated for

Table 2. GABA receptor density, maximal current, desensitization, and cellular capacitance in rat thalamic and cortical neurons

Age	Brain area	Current density (pA/μm^2)	Maximal current (pA)	Capacitance (pF)	% Desensitization
p5–p8	Cortex	1.6 ± 0.1	2454 ± 152	15.4 ± 1.0	26.2 ± 1.7
		(n = 12)	(n = 12)	(n = 12)	(n = 11)
	Thalamus	1.6 ± 0.2	2499 ± 197	16.2 ± 1.8	36.3 ± 4.1
		(n = 7)	(n = 7)	(n = 7)	(n = 10)
p18–p25	Cortex	1.8 ± 0.2	2229 ± 165	13.4 ± 1.4	29.1 ± 2.4
		(n = 12)	(n = 12)	(n = 12)	(n = 11)
	Thalamus	1.8 ± 0.2	2242 ± 246	12.5 ± 0.7	36.5 ± 2.3
		(n = 13)	(n = 13)	(n = 13)	(n = 16)
p60–75	Cortex	2.1 ± 0.2	2036 ± 213	10.7 ± 1.1	21.9 ± 3.4
		(n = 15)	(n = 15)	(n = 15)	(n = 13)
	Thalamus	2.0 ± 0.3	2210 ± 102	12.5 ± 1.3	32.5 ± 3.8
		(n = 11)	(n = 11)	(n = 11)	(n = 9)

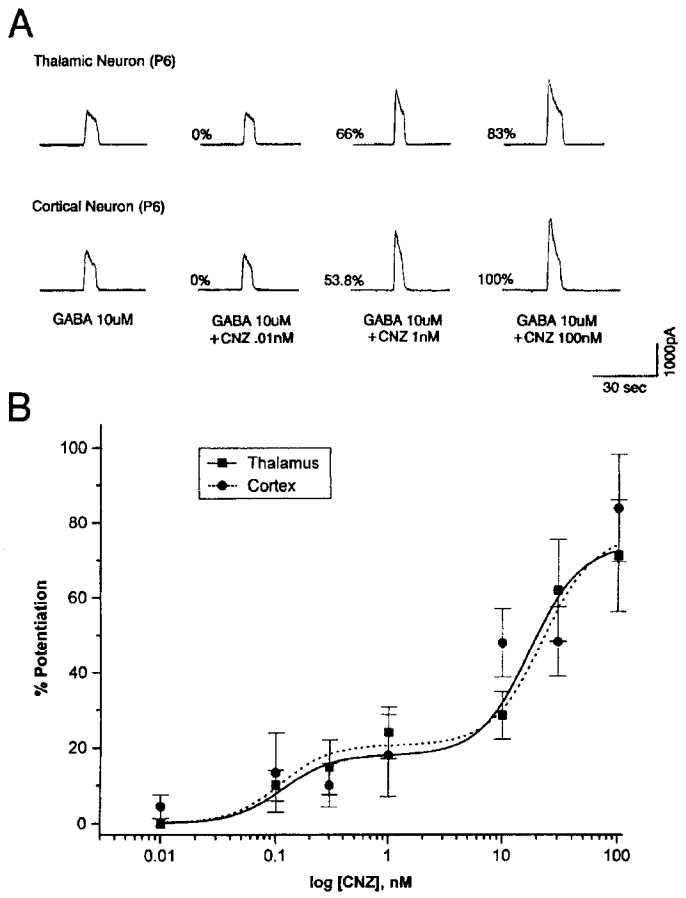

Figure 5. Clonazepam augmentation of GABA currents in p5–p8 rat thalamic and cortical neurons. *A*, Traces illustrating the augmentation of the control GABA response (*leftmost set of traces*) by three concentrations of clonazepam (*CNZ*; *right three sets of traces*) in a thalamic (*top*) and cortical (*bottom*) neuron. The concentrations of GABA and CNZ applied to elicit a given trace appear below the bottom traces. Note the concentration-dependent augmentation in amplitude of the current evoked by 10 μM GABA application by 0.01, 1, and 100 nM clonazepam. Also note that the overall augmentation in GABA-current amplitude elicited by 100 nM CNZ was similar in cortical and thalamic neurons. Both neurons are from the same p6 animal. *B*, Log/linear plot of the concentration of clonazepam applied during 10 μM GABA exposure against the mean ± 1 SE response, expressed as a percentage of the response to GABA 10 μM alone in the same neuron. Curves are unbiased nonlinear least squares of the data (fit parameters are in Table 3). Note the similar high-affinity clonazepam augmentation of GABA responses in p5–p8 cortical and thalamic neurons, and that the overall efficacy of clonazepam in potentiating GABA currents in cortical neurons was similar to that in thalamic neurons.

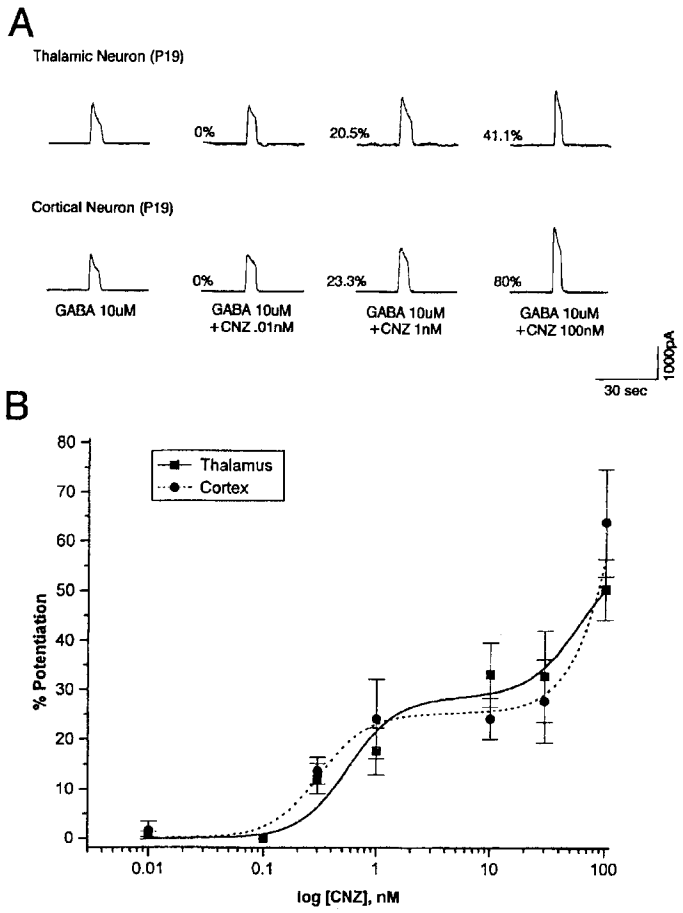

Figure 6. Clonazepam augmentation of GABA currents in p18–p25 rat thalamic and cortical neurons. *A* Traces illustrating the augmentation of the control GABA response (*leftmost set of traces*) by three concentrations of clonazepam (*CNZ*; *right three sets of traces*) in a thalamic (*top*) and cortical (*bottom*) neuron. The concentrations of GABA and CNZ applied to elicit a given trace appear below the bottom traces. Note the concentration-dependent increase in the amplitude of the current evoked by 10 μM GABA application by 0.01, 1, and 100 nM clonazepam. Also note that the overall increase in GABA-current amplitude evoked by 100 nM CNZ was larger in cortical neurons. Both neurons are from the same p19 animal. *B*, Log/linear plot of the concentration of clonazepam applied during 10 μM GABA exposure against the mean ± 1 SE response, expressed as a percentage of the response to GABA 10 μM alone in the same neuron. Curves are unbiased nonlinear least squares of the data (fit parameters are in Table 3). Note the similar high-affinity clonazepam augmentation of GABA responses in p18–p25 cortical and thalamic neurons, and that the overall efficacy of clonazepam in potentiating GABA currents in cortical neurons was not significantly greater than in thalamic neurons.

each neuron recorded (this drift could be due to either drift in amplitude or desensitization of GABA currents), and then the effect of this error calculated and temporally corrected for each GABA application, with or without benzodiazepine present. This drift was usually quite small. Neurons in which the drift rate exceeded a 5%/min were not analyzed.

Once drift rate corrections had been applied to each GABA exposure in a neuron, the effect of the benzodiazepine clonazepam on GABA-induced Cl^- currents was examined, by dividing the amplitude of a GABA current elicited in the presence of a given concentration of clonazepam by the amplitude of the control GABA current, without clonazepam present, and multiplying the resultant figure by 100, to convert it to a percentage. Using these methods of calculating potentiation, it was found that application of clonazepam in concentrations from 0.01 to 100 nM resulted in a concentration-dependent, sigmoidally increasing potentiation of GABA current amplitude for all developmental ages and cell types (Figs. 5–7). Above 100 nM, clonazepam-induced augmentation of GABA currents decreased, as has been reported previously (e.g., Yakushiji et al., 1993).

The results of nonlinear least squares analysis of the clonazepam potentiation of the GABA-induced currents in cortical and thalamic neurons during development are shown in Table 3. Fits of the data assuming a single binding site always exhibited a systematic error, with too much potentiation apparent for low

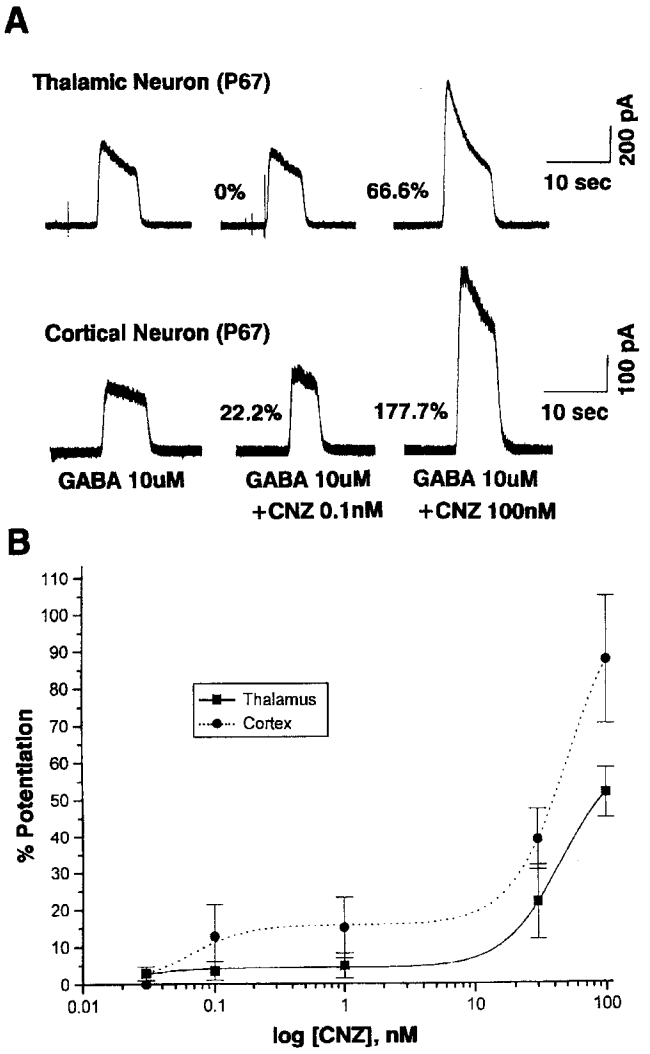

Figure 7. Clonazepam augmentation of GABA currents in adult (p60–75) rat thalamic and cortical neurons. *A*, Traces illustrating the augmentation of the control GABA response (*leftmost set of traces*) by two concentrations of clonazepam (*CNZ*; *right two sets of traces*) in a thalamic (*top*) and cortical (*bottom*) neuron. The concentrations of GABA and CNZ applied to elicit a given trace appear below the bottom traces. Note the concentration-dependent increase in the amplitude of the current evoked by 10 μM GABA application by 0.1 and 100 nM clonazepam. Also note that the overall increase in GABA-current amplitude evoked by 100 nM CNZ was larger in cortical neurons, and the potency of clonazepam was higher in cortical neurons, which showed significant potentiation in response to 0.1 nM CNZ, which had no effect on the thalamic neuron. Both neurons are from the same p67 animal. *B*, Log/linear plot of the concentration of clonazepam applied during 10 μM GABA exposure against the mean ± 1 SE response, expressed as a percentage of the response to GABA 10 μM alone in the same neuron. Curves are unbiased nonlinear least squares of the data (fit parameters are in Table 3). Note that augmentation of GABA responses by clonazepam in cortical neurons was greater throughout the curve, indicating increases in CNZ efficacy at both the high- and low-affinity sites in cortical neurons relative to thalamic neurons.

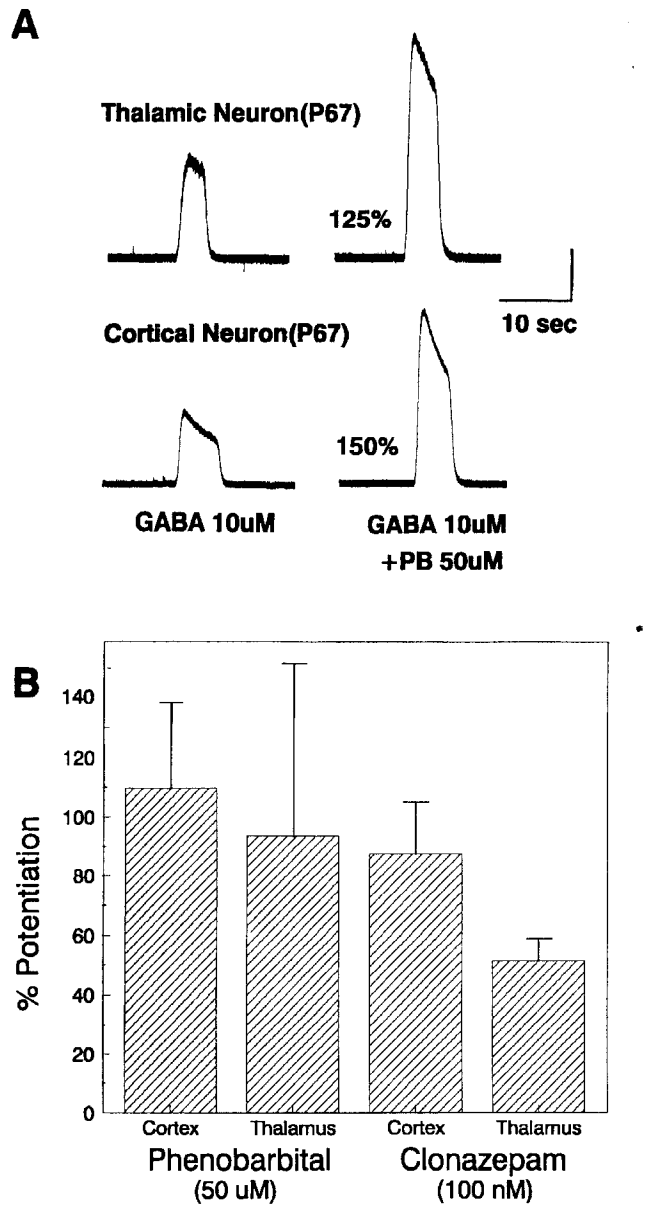

Figure 8. Phenobarbital augmentation of GABA currents in adult (p60–p75) thalamic and cortical neurons. *A*, Traces illustrating the augmentation of the response to GABA 10 μM by 50 μM phenobarbital in a thalamic (*top*) and a cortical neuron (*bottom*). Note the similar effect of phenobarbital on these two cells. Both cells were from the same animal, a p67 rat. Calibration: thalamus (*top*), 1 nA; cortex (*bottom*), 2 nA. *B*, Histogram illustrating the mean ± 1 SE augmentation of GABA currents in adult rat thalamic and cortical neurons by 50 μM phenobarbital, and by 100 nM clonazepam. Note the similar effect of phenobarbital in cortical and thalamic neurons, and that the overall efficacy of phenobarbital was similar to that seen with clonazepam in cortical, but not thalamic neurons.

concentrations of clonazepam. Therefore, a two-site model was employed to fit the data. This fit assumes two pharmacologically distinct binding sites for clonazepam, each with its own effect in potentiating GABA currents. The equation used to fit the clonazepam concentration/GABA augmentation curves was

$$\% \text{ Potentiation} = [M_1C^2/(C^2 + K_{D1}^2)] + [M_2C^2/(C^2 + K_{D2}^2)], \quad (2)$$

where M_1 and M_2 are the maximal effects for the high- and low-affinity sites, C is the concentration of clonazepam, and K_{D1} and K_{D2} are the clonazepam concentrations at which a half-maximal effect is seen for the high- and low-affinity sites, respectively. To increase the power of the fitting function, the Hill coefficient was fixed as 2, a value determined to be close to the actual value from preliminary fits of the data. Previous studies have found Hill coefficients of between 1 and 2 for clonazepam augmentation of GABA currents (Pritchett et al., 1989; Yakushiji et al.,

Table 3. Concentration/response fit parameters for clonazepam augmentation of GABA-induced currents in cortical and thalamic neurons

	Cortex				Thalamus			
Age	M_1	K_{D1}	M_2	K_{D2}	M_1	K_{D1}	M_2	K_{D2}
p5–p8	20.8 ± 11.4	0.11 ± 0.17	58.9 ± 17.5	20.0 ± 13.8	20.1 ± 3.3	0.11 ± 0.05	54.6 ± 5.0	19.2 ± 3.8
p18–p25	23.4 ± 2.9	0.27 ± 0.08	61.8 ± 21.8	75.0 ± 38.2	28.0 ± 6.9	0.55 ± 0.15	25.1 ± 9.5	40.1 ± 30.5
p60–p76	15.8 ± 3.3	0.06 ± 0.03	90.7 ± 8.0	51.2 ± 9.0	4.4 ± 0.6	0.02 ± 0.01	57.0 ± 1.4	45.2 ± 2.1

All values are ±1 SE M_1 and K_{D1} are the maximal effect and K_D values for the high-affinity clonazepam response, and M_2 and K_{D2} are the maximal effect and K_D values for the lower-affinity clonazepam response. All fits were conducted assuming a Hill coefficient of 2 for clonazepam augmentation of GABA currents for both the high- and low-affinity responses. Number of neurons recorded: p5–p8, 45 cortex, 54 thalamus; p18–p25, 29 cortex, 39 thalamus; p60–p74, 36 cortex, 37 thalamus.

1993), with the latter study reporting a Hill coefficient of 1.87 for diazepam potentiation of $GABA_A$ currents in p13–p17 acutely isolated rat neocortical neurons. When clonazepam concentration/GABA augmentation curves were fitted in the present study assuming only a single effective site, Hill coefficients were determined to be between 0.5 and 1 under these constraints (not shown), since the high-affinity effects also tended to make the slope of the plots "shallower." However, these fits were clearly inadequate, and so a two-site model was employed to fit the data.

A high-affinity site, with a K_D in the subnanomolar range (varying between 0.03 and 0.55 nM) contributed approximately 15–20% potentiation for most ages and cell types, and this maximal effect of the high-affinity site varied with cell type and age (Table 2). The efficacy (maximal augmentation) of this high-affinity site decreased with the age of the animal in thalamic neurons, with a maximal effect of 20.1% potentiation in p5–p8 neurons, decreasing to a 4.4% maximal effect in thalamic neurons from adult animals (Table 3, Figs. 5–7). In contrast, the high-affinity site efficacy remained relatively constant for cortical neurons across all ages (Table 3, Figs. 5–7). The low-affinity clonazepam site contributed a much greater maximal potentiation to the total effect of clonazepam, contributing 91% potentiation in adult (p60–p74) cortical neurons, and 57% total potentiation in adult thalamic neurons (Table 3, Fig. 7). In cortical neurons, low-affinity site efficacy increased gradually with development (Table 3). This was not the case in thalamic neurons, which showed a transient dip in efficacy at the low-affinity site in p18–p25 neurons (Table 3).

Phenobarbital augmentation of adult cortical and thalamic neurons GABA currents

Figure 8 shows phenobarbital effects on adult thalamic and cortical neurons. Phenobarbital augmented currents evoked by application of 10 μM GABA equally in cortical and thalamic neurons, with equivalent overall efficacy to maximal potentiation of GABA responses by clonazepam in adult cortical (but not thalamic) neurons (Fig. 8*B*).

Discussion

Results from the present study demonstrate regional and developmental differences in the function of $GABA_A$ receptors of somatosensory thalamic and cortical neurons, which could facilitate understanding of GABAergic mechanisms operative in the generation of normal and pathological rhythms in the thalamocortical system.

GABA responses

At all developmental stages, cortical neurons exhibited greater desensitization than did thalamic neurons, and desensitization increased in cortical (but not thalamic) neurons with postnatal development (Table 2). The K_D and Hill coefficient values derived from kinetic fits of the GABA concentration/response relationships varied with both postnatal age and cell type. In thalamus, the relative potency of GABA was p18–p25 = p60–p74 > p5–p8, while in cortical neurons GABA potency order was p18–p25 > p5–p8 > P60–p74 (Figs. 2–4, Table 1). The slope of the concentration/response curve was steepest in mid-postnatal development (p18–p25; Table 1). Hill coefficient values decreased in adult neurons to early postnatal levels in cortex, and to a level intermediate between p5–p8 and p18–p25 values in adult thalamic neurons (Table 1).

Several factors could affect the desensitization rate, potency, and slope of the GABA concentration/response relationship. One factor that could mediate these types of kinetic differences in $GABA_A$ responses is the structure of the $GABA_A$ receptors present on differing neuron types of varying ages. In functional studies of expressed $GABA_A$ receptor subunits in *Xenopus* oocytes (Sigel et al., 1990), human embryonic kidney cell lines (Verdoorn et al., 1990), or mouse fibroblasts (Angelotti and Macdonald, 1993), altering the subunit composition of the expressed GABA receptor has been shown to affect GABAergic potency (Sigel et al., 1990; Verdoorn et al., 1990), Hill coefficient (Sigel et al., 1990), single-channel conductance (Angelotti and Macdonald, 1993), and desensitization rate (Verdoorn et al., 1990). Receptors consisting of α and β subunits (but no γ subunit) had lower K_D values, lower Hill coefficients, lower single-channel conductances, and faster desensitization rates than receptors composed of α, β, and γ subunits. Therefore, one possible explanation for the altered kinetic properties of GABA in adult cortical neurons compared to thalamic neurons is that cortical neurons may have a higher proportion of GABA receptors containing a γ_2 subunit than thalamic neurons (e.g., Olsen et al., 1990; Wisden et al., 1992), which may result in this relative difference in GABA potency.

In situ hybridization studies examining expression of GABA subunit mRNAs provide evidence concerning which receptor subunits may be present in both adult (Persohn et al., 1992; Wisden et al., 1992) and developing (Laurie et al., 1992) rat brain. The cortex of adult rat brain shows a laminar specificity of expression of various GABA subunit mRNAs, with positive staining for α_1–α_4, β_2, β_3, and γ_2 subunits (Persohn et al., 1992; Wisden et al., 1992). In contrast, adult thalamus stains positively for only α_1, α_4, β_2, and δ subunits (Persohn et al., 1992; Wisden et al., 1992). The relative levels of expression of γ_2 mRNA subunits in the thalamus are controversial, with some studies finding little staining (Wisden et al., 1992) and others finding higher levels of γ_2 staining (Araki et al., 1992; Persohn et al., 1992).

The postnatal development of various GABA subunit mRNAs

shows a varying pattern when compared to adult mRNA (Laurie et al., 1992). Assuming that strength of mRNA hybridization staining corresponds to the amount of functional protein expressed, GABA responses in p5–p8 cortical neurons were probably due to activation of GABA receptors composed of $\alpha_{(2,3,or5)}\beta_{(2or3)}\gamma_2$, and in p5–p8 thalamic neurons of $\alpha_{(2-5)}\beta_3\gamma_1$ (Laurie et al., 1992). Some of the differences seen could therefore be due to alterations in subunit structure between the two brain areas, with the β_2 and γ_2 subunits absent in p5–p8 thalamic neurons but present in cortical neurons and the α_4 and γ_3 subunits present in thalamic neurons but absent in cortical neurons. By the same reasoning, GABA receptor responses in p18–p25 cortical neurons were probably due to activation of $\alpha_{(1-5)}$, $\beta_{(1-3)}$, γ_2 subunit–containing receptors (Laurie et al., 1992), with differences in GABA receptor function between p5–p8 and p18–p25 cortical neurons due to expression of α_1 and α_5, and β_1 subunits in p18–p25 neurons, which were not expressed similarly in p5–p8 cortical neurons. According to these mRNA expression data, thalamic neurons in the p18–p25 age range had GABA responses due to activation of $\alpha_{(1or4)}\beta_2\delta$ receptors (Laurie et al., 1992), with differences between p18–p25 and p5–p8 thalamic neuron GABA currents being explained by the addition of α_1, β_2, and δ subunits in p18–p25 neurons, and by the reduction in expression of $\alpha_{(2,3,or5)}$, β_3, and γ_1 subunits in p18–p25 thalamic neurons.

Benzodiazepine sensitivity

Benzodiazepine modulation of GABA receptor function showed the largest alterations in regional expression and postnatal development. Kinetic analysis in developing cortical and thalamic neurons (p5–p25) indicated that clonazepam acting on the high-affinity site had virtually identical effects within a given age group (Figs. 5, 6; Table 3). Clonazepam, acting at a lower-affinity site, was also equally effective in augmenting GABA responses in p5–p8 cortical neurons and thalamic neurons (Figs. 5, 6; Table 3). In p18–p25 neurons, clonazepam, acting at the low-affinity site, was more effective in cortical neurons than in thalamic neurons (62% compared to 25% augmentation; Table 3). In neurons from adult rats (>60 d old), this trend continued, with low-affinity site clonazepam effects augmenting GABA responses with greater efficacy in cortical neurons than in thalamic neurons (91% compared to 57%; Table 3). In adult thalamic neurons, the high-affinity site was reduced or absent, and the low-affinity site had a lower efficacy than that seen in cortical neurons. In adult cortical neurons, the high-affinity site accounted for 16% of the total efficacy of benzodiazepine receptors, with the remainder accounted for by the low-affinity site. Total augmentation (due to effects at both high- and low-affinity sites) was 107% in adult cortical neurons and 61% in thalamic neurons.

The reduced efficacy of clonazepam in potentiating GABA responses in thalamic relative to cortical neurons could be accounted for by two distinct mechanisms. Clonazepam could have differing effects at GABA receptors in thalamic and cortical neurons, or there could be a subset of thalamic GABA receptors that are insensitive to benzodiazepines, with neither of these mechanisms being mutually exclusive. Support for the former hypothesis is lent by recent findings that the sensitivity of GABA receptors containing a γ_2 subunit can be modulated depending on which α receptor subunits are present in the receptor (Pritchett et al., 1989). GABA receptors containing the α_1 subunit were found to display a BZ_1 receptor phenotype, while those containing α_2 or α_3 subunits were found to display a BZ_2 receptor phenotype (Pritchett et al., 1989). The expression of α receptor subunit mRNAs has been shown to vary depending on brain area, with distinct (but partially overlapping) populations of α receptor subunits expressed in thalamus and cortex (discussed above). Support for the latter hypothesis (a subset of thalamic GABA receptors present that are insensitive to benzodiazepines) is lent by a number of recent studies. Olsen et al. (1990) in binding studies have shown that there is a marked disparity between the number of high-affinity GABA binding sites and the number of benzodiazepine receptors in thalamus, suggesting that there could be a significant population of GABA receptors within thalamus (perhaps 80%) that do not bind benzodiazepines, and hence are not benzodiazepine modulated. Wisden et al. (1992) have shown that expression of γ_2 mRNA is reduced or absent in thalamus in adult rats (but see Araki et al., 1992; Persohn et al., 1992). This subunit has been shown in functional expression studies to confer benzodiazepine sensitivity to GABA receptors (Sigel et al., 1990), although the binding site for benzodiazepine appears to be contained within the α subunit (Pritchett and Seeburg, 1991). Therefore, alterations in benzodiazepine sensitivity in thalamus relative to cortex in adults are probably due to a combination of factors, including (1) thalamic GABA receptors, which are insensitive to benzodiazepines, explaining the overall decreased efficacy of benzodiazepines in thalamus relative to cortex, and (2) a population of GABA receptors in thalamic neurons that have altered modulatory responses or sensitivity to benzodiazepine binding, which could explain the altered kinetic properties of benzodiazepine potentiation of GABA responses in thalamus relative to cortex.

The increased efficacy of benzodiazepines at cortical $GABA_A$ receptors of adult animals relative to thalamic GABA receptors has therapeutic significance. The anticonvulsant activity of both benzodiazepines and barbiturates is thought to be mediated to a large extent by allosteric enhancement of GABAergic inhibition (Schulz and Macdonald, 1981; Macdonald and McLean, 1986; Twyman et.al., 1989). Barbiturates, unlike benzodiazepines, are equally effective in augmenting GABA responses in both cortical and thalamic neurons (Fig. 8). Barbiturates, unlike benzodiazepines (which are effective GA anticonvulsants; Browne and Penry, 1973; Dreifuss et al., 1975), are ineffective or may even exacerbate GA (Penry and So, 1981), a seizure disorder that involves activation of rhythmic thalamocortical oscillations. This tendency of barbiturates to activate thalamocortical rhythms is particularly evident in barbiturate-anesthetized animals, which typically generate spontaneous thalamocortical oscillations resembling SSs (e.g., Andersen et al., 1967). Since GABAergic IPSPs in thalamic neurons function to synchronize thalamocortical oscillations, augmenting these IPSPs would enhance (or exacerbate) rhythmicity, as has been seen in animal models of GA (Liu et al., 1991). Cortical neurons have much smaller proportional low-threshold calcium current compared to thalamic neurons (cf. Coulter et al., 1989a–c; Sayer et al., 1990), and so do not tend to be paradoxically activated by hyperpolarization as do thalamic neurons. Therefore, augmenting cortical GABAergic inhibition has a net effect of reducing excitability. Examining cortical and thalamic effects of barbiturates and benzodiazepines on GABA receptor function can help explain their contrasting actions in controlling GA. Benzodiazepines would potentiate GABAergic IPSPs in neocortex to a greater extent than in thalamus (e.g., Fig. 7), while barbiturates are equally effective in both areas (Fig. 8). Aug-

mentation of GABAergic function in thalamus would tend to promote rhythm generation, confounding anticonvulsant actions in cortex, and reducing the relative effectiveness of barbiturates as GA anticonvulsants. A recent report has appeared describing indirect evidence that clonazepam also may have actions in NRT, serving to increase intra-NRT recurrent IPSPs, and reducing NRT-mediated inhibition of thalamic neurons, an action also consistent with anticonvulsant effectiveness of this drug in controlling GA epilepsy (Huguenard and Prince, 1994). Determination of the effects of barbiturates on intra-NRT recurrent inhibition awaits further study.

References

Andersen P, Sears TA (1964) The role of inhibition in the phasing of spontaneous thalamo-cortical discharge. J Physiol (Lond) 173:459–480.

Andersen P, Andersson SA, Lømo T (1967) Some factors involved in the thalamic control of spontaneous barbiturate spindles. J Physiol (Lond) 192:257–281.

Angelotti TP, Macdonald RL (1993) Assembly of $GABA_A$ receptor subunits: $\alpha_1\beta_1$ and $\alpha_1\beta_1\gamma_{2S}$ subunits produce unique ion channels with dissimilar single-channel properties. J Neurosci 13:1429–1440.

Araki T, Sato M, Kiyama H, Manabe Y, Tohyama M (1992) Localization of $GABA_A$ γ_2-subunit mRNA-containing neurons in the rat central nervous system. Neuroscience 47:45–61.

Barker JL, Harrison NL (1988) Outward rectification of inhibitory postsynaptic currents in cultured rat hippocampal neurones. J Physiol (Lond) 403:41–55.

Bormann J, Hamill OP, Sakmann B (1987) Mechanism of anion permeation through channels gated by glycine and γ-aminobutyric acid in mouse cultured neurons. J Physiol (Lond) 385:243–286.

Bowery NG, Hudson AL, Price GW (1987) $GABA_A$ and $GABA_B$ receptor site distribution in the rat central nervous system. Neuroscience 20:365—383.

Browne TR, Penry JK (1973) Benzodiazepines in the treatment of epilepsy. Epilepsia 14:277–310.

Coulter DA, Huguenard JR, Prince DA (1989a) Calcium currents in rat thalamocortical relay neurones: kinetic properties of the transient, low-threshold current. J Physiol (Lond) 414:587–604.

Coulter DA, Huguenard JR, Prince DA (1989b) Characterization of ethosuximide reduction of low-threshold calcium current in thalamic neurons. Ann Neurol 25:582–593.

Coulter DA, Huguenard JR, Prince DA (1989c) Specific petit mal anticonvulsants reduce calcium currents in thalamic neurons. Neurosci Lett 98:74–78.

Coulter DA, Huguenard JR, Prince DA (1990a) Differential effects of petit mal anticonvulsants and convulsants on thalamic neurones: calcium current reduction. Br J Pharmacol 100:800–806.

Coulter DA, Huguenard JR, Prince DA (1990b) Differential effects of petit mal anticonvulsants and convulsants on thalamic neurones: GABA current blockade. Br J Pharmacol 100:807–813.

Deschênes M, Roy JP, Steriade M (1982) Thalamic bursting mechanism: a slow inward current revealed by membrane hyperpolarization. Brain Res 239:289–293.

Dreifuss FE, Penry JK, Rose CW, Kupferberg HJ, Dyken P, Sato S (1975) Serum clonazepam concentrations in children with absence seizures. Neurology 25:255–258.

Forscher P, Oxford GS (1985) Modulation of calcium channels by norepinephrine in internally dialyzed avian sensory neurons. J Gen Physiol 85:43–763.

Gloor P, Fariello RG (1988) Generalized epilepsy: some of its cellular mechanisms differ from those of focal epilepsy. Trends Neurosci 11: 63–68.

Goldman DE (1943) Potential, impedance, and rectification in membranes. J Gen Physiol 27:37–60.

Hamill OP, Marty A, Neher E, Sakmann B, Sigworth FJ (1981) Improved patch clamp technique for high resolution recordings from cells and cell-free membranes. Pfluegers Arch 391:85–100.

Hodgkin AL, Katz B (1949) The effects of sodium ions on the electrical potential of the giant axon of the squid. J Physiol (Lond) 108:37–87.

Hosford DA, Clark S, Cao Z, Wilson WA, Lin F, Morrisett RA, Huin A (1992) The role of $GABA_B$ receptor activation in absence seizures of lethargic (*lh/lh*) mice. Science 257:398–400.

Houser CR, Vaughn JE, Barber RP, Roberts E (1980) GABA neurons are the major cell type of nucleus reticularis thalami. Brain Res 200: 341–354.

Huguenard JR, Alger BE (1986) Whole-cell voltage-clamp study of the fading of GABA-activated currents in acutely dissociated hippocampal neurons. J Neurophysiol 56:1–17.

Huguenard JR, Prince DA (1992) A novel T-type current underlies prolonged Ca^{2+}-dependent burst firing in GABAergic neurons of rat thalamic reticular nucleus. J Neurosci 12:3804–3817.

Huguenard JR, Prince DA (1994) Clonazepam suppresses $GABA_B$-mediated inhibition in thalamic relay neurons through effects in nucleus reticularis. J Neurophysiol 71:2576–2581.

Huguenard JR, Coulter DA, Prince DA (1991) A fast transient potassium current in thalamic relay neurons: kinetics of activation and inactivation. J Neurophysiol 66:1304–1315.

Jahnsen H, Llinás R (1984) Electrophysiological properties of guinea-pig thalamic neurones: an *in vitro* study. J Physiol (Lond) 349:205–226

Jones EG (1985) The thalamus. New York: Plenum.

Kay AR, Wong RKS (1986) Isolation of neurons suitable for patch clamping from adult mammalian nervous systems. J Neurosci Methods 16:227–238.

Laurie DJ, Wisden W, Seeburg PH (1992) The distribution of thirteen $GABA_A$ receptor subunit mRNAs in the rat brain. III. Embryonic and postnatal development. J Neurosci 12:4151–4172.

Liu Z, Vergnes M, Depaulis A, Marescaux C (1991) Evidence for a critical role of GABAergic transmission within the thalamus in the genesis and control of absence seizures in the rat. Brain Res 545:1–7.

Liu Z, Vergnes M, Depaulis A, Marescaux C (1992) Involvement of intrathalamic $GABA_B$ neurotransmission in the control of absence seizures in the rat. Neuroscience 48:87–93.

Llinás R, Jahnsen H (1982) Electrophysiology of mammalian thalamic neurones *in vitro*. Nature 297:406–408.

Macdonald RL, McLean MJ (1986) Anticonvulsant drugs: mechanisms of action. Adv Neurol 44:713–736.

Mody I, Salter MW, Macdonald JF (1988) Requirement for NMDA receptor/channels for intracellular high energy phosphates and the extent of intraneuronal calcium buffering in cultured mouse hippocampal neurons. Neurosci Lett 93:73–78.

Newland CF, Colquhoun D, Cull-Candy SG (1991) Single channels activated by high concentrations of GABA in superior cervical ganglion neurones of the rat. J Physiol (Lond) 432:203–233.

Olsen RW, Tobin AT (1990) Molecular biology of $GABA_A$ receptors. FASEB J 4:1469–1480.

Olsen RW, McCabe RT, Wamsley JK (1990) $GABA_A$ receptor subtypes: autoradiographic studies of GABA, benzodiazepine, and convulsant binding sites in the rat central nervous system. J Chem Neuroanat 3:59–76.

Penry JK, So E (1981) Refractoriness of absence seizures and phenobarbital. Neurology 31:158.

Persohn E, Malherbe P, Richards JG (1992) Comparative molecular neuroanatomy of cloned $GABA_A$ receptor subunits in the rat CNS. J Comp Neurol 326:193–216.

Pritchett DB, Seeburg PH (1991) γ-Aminobutyric acid type A receptor point mutation increases the affinity of compounds for the benzodiazepine site. Proc Natl Acad Sci USA 88:1421–1425.

Pritchett DB, Sontheimer H, Shivers BD, Ymer S, Kettenmann H, Schofield PR, Seeburg P (1989) Importance of a novel $GABA_A$ receptor subunit for benzodiazepine pharmacology. Nature 338:582–585.

Purpura DP, Cohen B (1962) Intracellular recording from thalamic neurons during recruiting responses. J Neurophysiol 25:621–635.

Sayer RJ, Schwindt PC, Crill WE (1990) High- and low-threshold calcium currents in neurons acutely isolated from rat sensorimotor cortex. Neurosci Lett 120:175–178.

Schulz DW, Macdonald RL (1981) Barbiturate enhancement of GABA-modulated inhibition and activation of chloride ion conductance: correlation with anticonvulsant and anesthetic actions. Brain Res 209: 177–188.

Segal M, Barker JL (1984) Rat hippocampal neurons in culture: properties of GABA-activated Cl-ion conductance. J Neurophysiol 51: 500–515.

Sigel E, Baur R, Trube G, Möhler H, Malherbe P (1990) The effect

of subunit composition of rat brain $GABA_A$ receptors on channel function. Neuron 5:703–711.

Stelzer A, Kay AR, Wong RKS (1988) GABA-receptor function in hippocampal cells is maintained by phosphorylation factors. Science 242:339–341.

Steriade M, Llinás RR (1988) The functional states of the thalamus and the associated neuronal interplay. Physiol Rev 68:649–742.

Steriade M, Deschênes M, Domich L, Mulle C (1985) Abolition of spindle oscillations in thalamic neurons disconnected from nucleus reticularis thalami. J Neurophysiol 54:1473–1497.

Steriade M, Domich L, Oakson G, Deschênes M (1987) The deafferented nucleus reticularis generates spindle rhythmicity. J Neurophysiol 57:260–273.

Twyman RE, Rogers CJ, MacDonald RL (1989) Differential regulation of γ-aminobutyric acid receptor channels by diazepam and phenobarbital. Ann Neurol 25:213–220.

Verdoorn TA, Draguhn A, Ymer S, Seeburg PH, Sakmann B (1990) Functional properties of recombinant $GABA_A$ receptors depend upon subunit composition. Neuron 4:919–928.

Wisden W, Laurie DJ, Monyer H, Seeburg PH (1992) The distribution of 13 $GABA_A$ receptor subunit mRNAs in the rat brain. I. Telencephalon, diencephalon, mesencephalon. J Neurosci 12:1040–1062.

Yakushiji T, Shirasaki T, Munakata M, Hirata A, Akaike N (1993) Differential properties of type I and type II benzodiazepine receptors in mammalian CNS neurones. Br J Pharmacol 109:819–825.

Yellen G (1982) Single Ca^{2+}-activated non-selective cation channels in neuroblastoma cells. Nature 296:357–359.